


Article

# Binary Liquid Crystal Mixtures Based on Schiff Base Derivatives with Oriented Lateral Substituents

Rua B. Alnoman<sup>1</sup>, Mohamed Hagar<sup>1,2,\*</sup>, Hoda A. Ahmed<sup>3,\*</sup> , Magdi M. Naoum<sup>3</sup>, Hanefah A. Sobaih<sup>1</sup>, Jawaher S. Almshaly<sup>1</sup>, Mawadh M. Haddad<sup>1</sup>, Rana A. Alhaisoni<sup>1</sup> and Tahani A. Alsobhi<sup>1</sup>

<sup>1</sup> Chemistry Department, College of Sciences, Taibah University, Yanbu 30799, Saudi Arabia; rua-b-n@live.co.uk (R.B.A.); Tu3750343@taibahu.edu.sa (H.A.S.); Tu3754203@taibahu.deu.sa (J.S.A.); Tu3753759@taibahu.edu.sa (M.M.H.); Tu3754163@taibahu.edu.sa (R.A.A.); Tu3754147@taibahu.edu.sa (T.A.A.)

<sup>2</sup> Faculty of Science, Chemistry Department, Alexandria University, Alexandria 21321, Egypt

<sup>3</sup> Faculty of Science, Department of Chemistry, Cairo University, Cairo 12613, Egypt; magdinaoum@yahoo.co.uk

\* Correspondence: mhagar@taibahu.edu.sa (M.H.); ahoda@sci.cu.edu.eg (H.A.A.)

Received: 30 March 2020; Accepted: 15 April 2020; Published: 20 April 2020



**Abstract:** Binary mixtures of the laterally substituted Schiff base/ester derivatives, namely 4-((2- or 3-) substituted phenyl imino methyl) phenyl-4''-alkoxy benzoates, Ia–d, were prepared and mesomorphically studied by differential scanning calorimetry (DSC) and their mesophases identified by polarized optical microscopy (POM). The lateral group (1-naphthyl, 2-F, 2-Br, 3-F in Ia–d, respectively) is attached to different positions of the phenyl Schiff moiety. The mixtures investigated were made from two differently shaped compounds that differ from each other in the polarity, size, orientation, and relative positions of the lateral group. The results revealed that the binary mixture Ia/Ib (bearing the naphthyl and 2-flouro substituents) exhibited the SmA phase, which covered the whole composition range. For the mixtures Ib/Id (2-F and 2-Br), the isomeric lateral F-group in compound Ib distributed the SmA arrangement of Id. In the Ic/Id mixture bearing two positionally and structurally different substituents, the addition of Ic to Id resulted in solid binary mixtures where its behavior may be attributed to the negligible steric effect of the small electronegative fluorine atom compared to the Br atom. Density functional theory (DFT) theoretical calculations were carried out to estimate the geometrical parameters of individual components and to show the effect of these parameters in the mesophase behavior of the binary system, where the higher dipole moment of Id (6 Debye) may be the reason for its high  $\pi$ – $\pi$  molecular stacking, which influences its mesophase range and stability.

**Keywords:** binary phase diagram; lateral substituent; Schiff base liquid crystals; induced phases; DFT

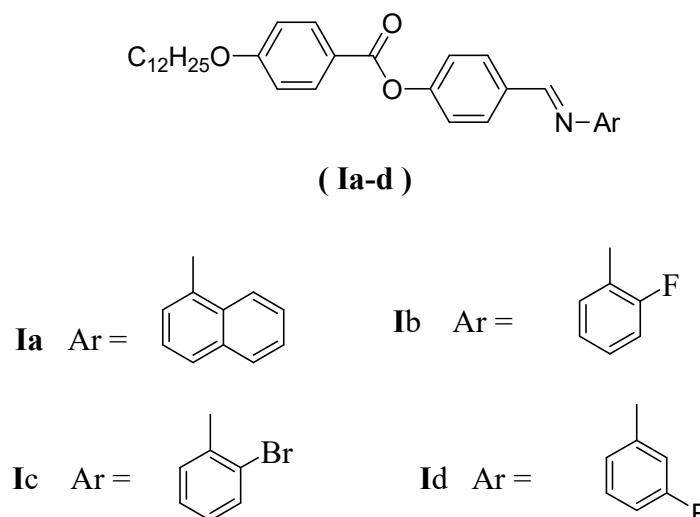
## 1. Introduction

Due to their favorable characteristics, liquid crystals can act as an important component in various applications such as liquid crystal displays, solar cells, sensors, modulators, etc. [1]. Additionally, liquid crystals are useful in medicine, biology, food production, and for oil recovery. Therefore, the design and development of liquid crystalline systems have gained considerable research interest over the past decade [2–5]. Liquid crystalline materials are classified into three distinct types: polymeric, lyotropic, and thermotropic. Thermotropic liquid crystals have been widely studied and used for their linear and nonlinear optical properties [2,6–18]. Usually, this type of liquid crystal is represented as rigid rods, which can interact with one another and form characteristic ordered structures. It is already

known that the mesomorphic characteristics of liquid crystalline compounds are strongly affected when a lateral substituent is appended into their mesogenic cores [19–21]. The extent of change is dependent on the size, orientation, and polarity of the lateral group. Sterically, a lateral substituent widens the core and increases the intermolecular separation, which leads to the reduction in the lateral interactions [19–21] and hence the mesomorphic stability is slightly reduced. Thus, the incorporation of the lateral group in the skeleton of a liquid crystalline molecule makes the molecules broad, thus lateral substitution plays an important role in its mesogenic properties. Recently, one of our interests has been to correlate the molecular geometry of mesogens with their mesophase behavior. Later, we investigated several Schiff base/ester liquid crystal derivatives [13,22,23]. Mesomorphic behavior of mesogenic groups may be greatly modified upon the mixing of individual compounds. It is well known that forming a mixture of two or more liquid crystal components leads to tuning the needed properties of interest [24–33]. An example is the mixing of two non-mesomorphic compounds in order to reduce its melting point, which has gained wide use in many applications. Thus, liquid crystal mixtures show phase transition temperatures and physical properties that differ from their constituents.

The binary mixture of liquid crystalline materials could be better constructed for certain applications in many fields, rather than the individual components [34]. Consequently, the investigation of mesomorphic properties of such mixtures is of considerable interest [35–37]. These types of mixtures have been shown to achieve liquid crystalline materials of lower melting point [38–40]. In addition, due to the straight or slightly enhanced mesophase-to-isotropic line, the mesophase range is greater for the eutectic mixture than for either its pure components.

The aim of our present study was to prepare three binary systems of differently laterally substituted derivatives bearing the same terminal flexible core, but of lateral naphthyl (Ia), 2-F (Ib), 2-Br (Ic), and 3-F (Id) in order to investigate their mesomorphic and optical activities (Scheme 1). The lateral group protruded with different size, polarity, and position with respect to the Schiff base core, which was connected to the other terminal benzene ring attached to the azomethine moiety, was also investigated. Finally, a brief study of the thermal and geometrical parameters of pure components by DFT calculations were conducted and correlated with the experimental values of their mixed states.



Scheme 1. Investigated compounds Ia-d.

## 2. Experimental

### 2.1. Materials and Preparation of Binary Mixtures

Compounds used in this study were synthesized and characterized according to the methods attached as Supplementary Materials.

Binary mixtures were prepared by mixing accurately weighed samples of the appropriate amounts of the individual components ( $\pm 1.0\%$  in composition), melting them together to give an intimate mixture, and then cooled to room temperature while stirring.

For the construction of the binary phase diagram, the mixtures of any two components were made to cover the whole range of composition.

## 2.2. Physical Characterization

Calorimetric measurements were carried out using a TA Instruments Co. Q20 differential scanning calorimetry (DSC; Waltham, MA, USA). The DSC was calibrated using the melting temperatures and enthalpies of indium and lead. DSC investigations were carried out for small samples (2–3 mg) placed in aluminum pans. All measurements were achieved at a heating rate of  $10\text{ }^{\circ}\text{C}/\text{min}$  in an inert atmosphere of nitrogen gas (30 mL/min) and all transitions were recorded from the second heating scan.

Transition temperatures were checked and the types of mesophases identified for all compounds and mixtures investigated. Molar ratios of both components were melted and mixed to form intimate blends, then cooled. The mixture was put between two glass plates and heated to obtain a very thin layer. The texture was observed under a polarized optical microscope (POM, Wild, Wetzlar, Germany). Temperature was recorded by a Brookfield temperature controller (Harlow, Essex, England), England (Mettler FP82HT hot stage).

## 2.3. Computational Method and Calculations

The theoretical calculations were carried out by Gaussian 09 software (2009, Gaussian Inc.: Wallingford, CT, USA) [41]. The DFT/B3LYP method and 6–31G (d,p) basis set were selected for the calculations. The structures of the optimized geometries were drawn with Gauss View [42].

## 3. Results and Discussion

### 3.1. Binary Mixtures Studies

Transition temperatures and their corresponding transition enthalpies for the three binary mixtures (Ia/Ib, Ib/Id, and Ic/Id) are presented in Table 1. Both components of all mixtures bear the same flexible alkoxy chains ( $n = 12$ ) connected to the phenyl ester moiety. Individual compounds were reported in our previous work [43]. Figure 1 shows the DSC thermograms of 80 mol% composition of Ib (at eutectic composition) for the binary mixture Ib/Id. All mixtures were subjected to second heating/cooling cycles. Representative textures under polarizing optical microscopy of the observed mesophases are shown in Figure 2. Phase transition behaviors are graphically established in Figures 3–5.

**Table 1.** Phase transition temperatures ( $^{\circ}\text{C}$ ) and enthalpy of transition  $\Delta H$ , kJ/g for binary mixtures% upon the second heating scan.

Compound	$T_{\text{Cr-SmA}}$	$\Delta H_{\text{Cr-SmA}}$	$T_{\text{Cr-N}}$	$\Delta H_{\text{Cr-N}}$	$T_{\text{SmA-I}}$	$\Delta H_{\text{SmA-I}}$	$T_{\text{SmA-N}}$	$\Delta H_{\text{SmA-N}}$	$T_{\text{N-I}}$	$\Delta H_{\text{N-I}}$
<b>System Ia/Ib</b>										
0% Ia	-	-	103.3	48.28					120.3	0.80
20% Ia	98.0	69.10					107.3	1.89	120.9	1.26
40% Ia	76.9	64.3					97.1	3.16	111.3	2.67
60% Ia	77.5	44.79					95.8	5.25	111.5	1.64
80% Ia	84.9	69.15					94.8	2.43	105.9	1.77
100% Ia			98.8	19.73					96.3 *	0.18
<b>System Ib/Id</b>										
0% Ib	88.9	45.69			140.2	5.10				
20% Ib	101.8	58.65					113.5	0.98	140.4	1.55

Table 1. Cont.

Compound	$T_{Cr-SmA}$	$\Delta H_{Cr-SmA}$	$T_{Cr-N}$	$\Delta H_{Cr-N}$	$T_{SmA-I}$	$\Delta H_{SmA-I}$	$T_{SmA-N}$	$\Delta H_{SmA-N}$	$T_{N-I}$	$\Delta H_{N-I}$
40% Ib	100.9	69.09					107.7	0.66	132.4	1.93
60% Ib			95.9	94.61					135.8	2.38
80% Ib			95.4	68.64					134.6	1.25
100% Ib			103.3	48.28					120.3	0.80
System Ic/Id										
0% Ic	88.9	45.69			140.2	5.10				
20% Ic	98.5	66.90					115.6	0.89	124.8	1.52
40% Ic			99.4	73.3					119.6	1.10
60% Ic			100.0	69.46					118.3	0.91
80% Ic			100.7	71.84					112.8	0.85
100% Ic			93.2	46.33					99.0	0.37

Cr-SmA denotes the transition from crystal to the SmA phase; Cr-N denotes the transition from crystal to the N phase; SmA-N denotes the transition from SmA to the N phase; N-I denotes the transition from N to the isotropic liquid phase; \* monotropic phase observed only on cooling.

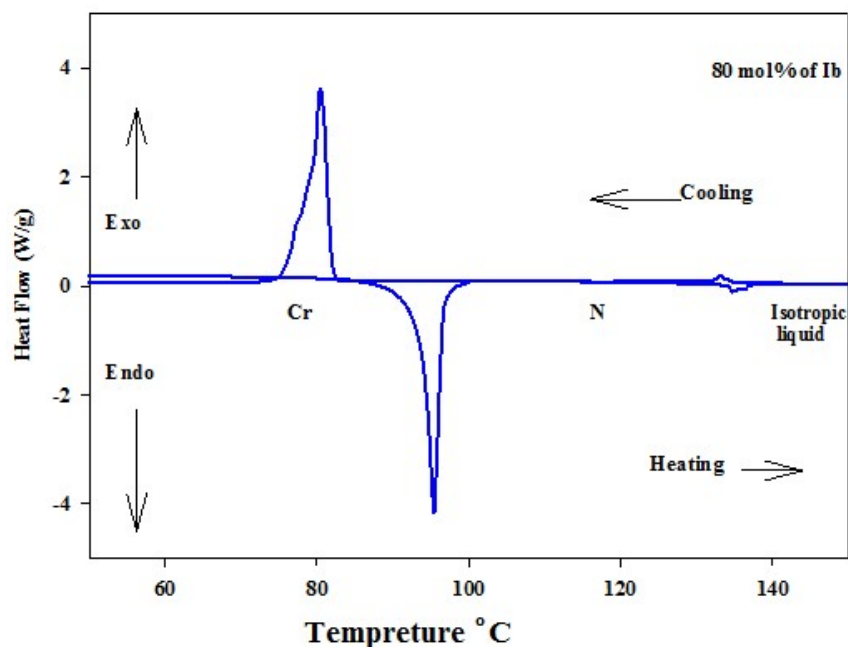


Figure 1. Differential scanning calorimetry (DSC) thermograms of binary mixture 80 mol% Ib for system Ib/Id upon the second heating/cooling cycles with a rate of 10 °C/min.

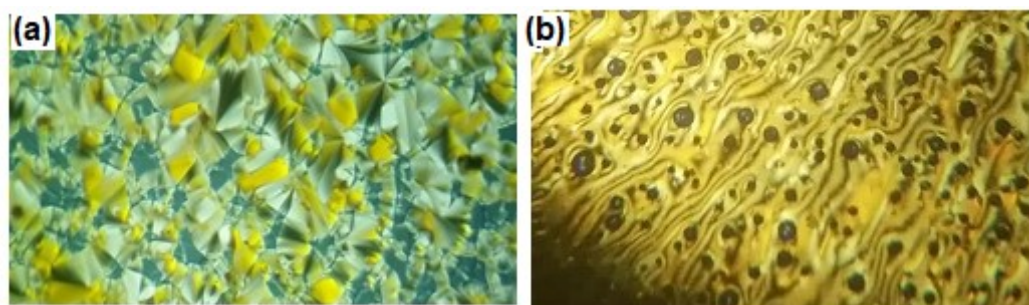
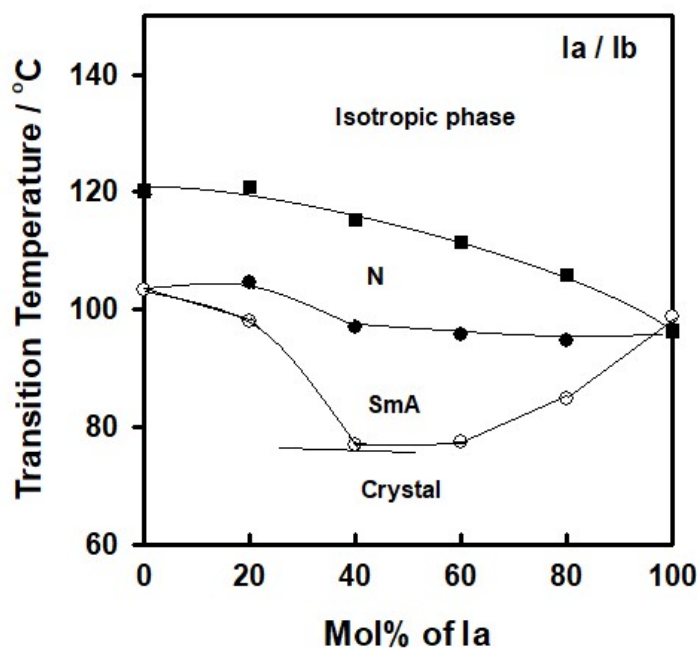


Figure 2. Polarized optical microscopy (POM) textures (the width of the images is about 40  $\mu$ m) of the binary mixture 40 mol% Ia for system Ia/Ib upon heating. (a) SmA phase at 86 °C; (b) N phase at 108 °C.

The phase diagrams of the binary mixtures are different depending on the type of its individual components. The variation in the polarity and/or the position of the lateral group is the main factors. The aim of such investigation was to attain a balance between the two components' mesomorphic properties, which is expected to be improved upon mixing, thus obtaining advantageous physical properties compared to the laterally substituted pure components (Ia–d).

### 3.1.1. Binary Phase Behavior of Mixtures of Analogues of Different Rigidity

In the first system, the binary phase diagram was made from the naphthyl derivative Ia and 2-F-substituted component Ib, and is illustrated in Figure 3. As can be seen from Table 1 and Figure 3, both the nematic and SmA stabilities varied regularly with the composition. Upon mixing the two components, enantiotropic dimorphic (SmA and N) phases covering the whole range of composition. The SmA mesophase was induced upon the addition of less than 20 mol% of Ia to the nematogenic component Ib. Their mixed solid phase exhibited eutectic behavior at about 40 mol% of Ia. The eutectic mixture of this system possessed a SmA temperature range ( $T_{\text{SmA-N}} - T_{\text{Cr-SmA}} = 20.2 \text{ }^\circ\text{C}$ ) and a N temperature range ( $T_{\text{N-I}} - T_{\text{SmA-N}} = 14.2 \text{ }^\circ\text{C}$ ). As concluded from the theoretical calculations, the two homologous Ia and Ib had different aspect ratios, in which the space filling of the naphthyl group was higher than that of the lateral fluorine atoms, thus may be located in the opposite directed structure; hence the addition of naphthyl derivative Ia is not expected to disturb the molecular arrangement of the lateral F-compound Ib. The N stability of both components is regularly affected upon mixing and was found to decrease with the mol% of Ia. A good induced SmA mesomorphic range covered the whole composition range of the mixture, which had a wide range at the eutectic composition (40 mol% of Ia).



**Figure 3.** Binary phase diagrams for system Ia/Ib; the symbol “o” denotes the solid–SmA phase, “●” the SmA–N phase transitions, “■” N–I phase transition upon second heating, and “—” denotes to eutectic mixture.

### 3.1.2. Binary Mixtures of the Analogues Bearing Substituent of the Same Polarity but of Different Orientation

The binary phase diagram of the laterally F-substituted isomers in different positions Ib/Id is represented graphically in Figure 4. The difference between the two isomers is the position (and/or orientation) of the small sized F-atom. Both analogues, again, bear the same terminal alkoxy chain

length ( $n = 12$ ), but differ in their type of mesophases. The first isomer Ib (2-F) is purely nematogenic with a narrow N phase range while the other isomer Id (3-F) possesses only the SmA phase. Examining their phase diagram (Figure 4) revealed that the addition of one isomer to the other was accompanied by a slight increase in temperature range as a result of the depression of its melting point upon mixing. All mixtures of the two components up to 60 mol% were enantiotropic dimorphic (SmA and N), whereas the SmA phase vanished at 60 mol % of Ib. The nematic phase covered all of the composition range. The eutectic mixture appeared around 80 mol % of Ib. As can also be seen from Figure 4, the N phase stability of Ib decreased gradually upon the addition of its isomer Id, which may be attributed to the difference in the orientation of the lateral F-atom in the individual components. The mesomorphic stabilities were mainly dependent upon the intermolecular attractions, in which the molecular polarity plays a significant role; it has been reported that the dipole moment of any compound is dependent upon the nature and orientation of the substituent [44].

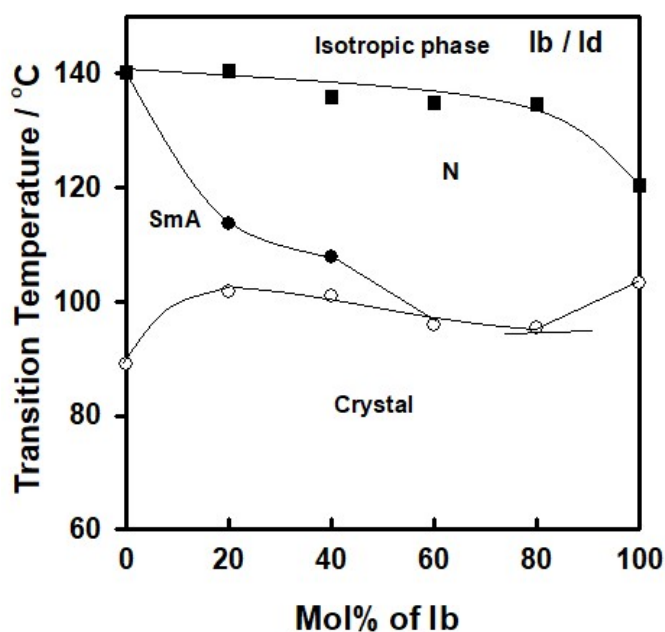


**Figure 4.** Binary phase diagrams for system Ib/Id; the symbol “o” denotes the solid–SmA phase, “●” the SmA–N phase transitions, “■” the N–I phase transition upon second heating, and “—” denotes the eutectic mixture.

### 3.1.3. Binary Mixtures of the Analogues Bearing Substituents of the Different Orientation and Different Size

The binary phase diagram of the mixtures 2-Br and 3-F substituted analogues Ic/Id was constructed and represented graphically in Figure 5. In such a system, the 3-F derivative is purely nematogenic, while the 2-Br analogue is purely smectogenic (SmA phase). Their mixtures showed no eutectic composition. Instead, their binary mixtures exhibited solid solutions throughout their composition range. In addition, the gradual decrease observed for the N and SmA mesophase stability indicated the good rearrangement of molecules of both isomers upon mixing either in their solid state or in the mesophase. This behavior may be attributed to the negligible steric effect of the small fluorine atom. Furthermore, the addition of the Ic to Id resulted in the disappearance of the SmA phase of Id upon the addition of about 40 mol % of Ic.

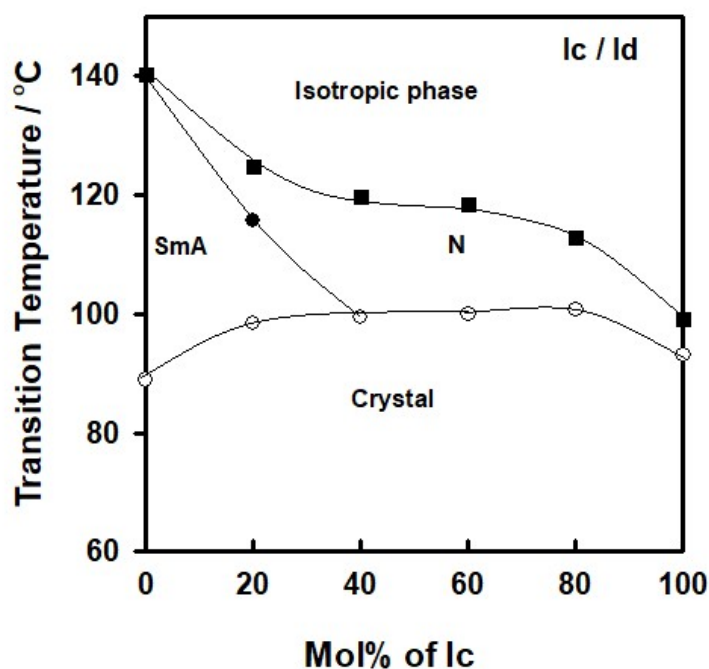


**Figure 5.** Binary phase diagrams for system Ic/Id; the symbol “o” denotes the solid–SmA phase, “●” the SmA–N phase transitions, and “■” is the N–I phase transition upon the second heating.

Generally, the dipole moment, polarizability, and aspect ratio greatly affect the competition between the lateral and end-to-end molecular attractions, which are important parameters influencing the mesomorphic behavior. Furthermore, the molecular architecture also affects the molecular–molecular interactions. In the present study, molecular aromatic  $\pi$ – $\pi$  stacking of rod-shaped liquid crystal molecules were observed due to the parallel attraction between co-planar molecules. Moreover, these interactions were enhanced by longer alkoxy-chains ( $n$ ). Another factor that could affect the mesophase behavior is the terminal aggregation of alkoxy chains (end-to-end association). This strong end-to-end association is the result of intermolecular interaction between the terminal alkoxy chains [38]. All these parameters share different ratios and resulted in improving the mesophase stability ( $T_c$ ), mesophase range, and type of individual components as well as their mixtures.

### 3.2. DFT Theoretical Calculations

The theoretical DFT estimations for the individual compounds Ia–d were calculated by DFT in a gas phase at the B3LYP 6–311G basis set. All optimum estimated structures were proven to have a stable geometry due to the absence of the imaginary frequency. Results of the theoretical DFT predictions of these compounds before mixing showed a non-co-planar geometrical with little twisted shape and with bent non-linear structure. The three phenyl rings of the individual compounds were completely planar, regardless of the type of mesogenic core. Recently, it was reported that the mesomorphic behavior of liquid crystalline (LC) materials highly depends on the geometrical structure [7,9,12,45–47]. Moreover, one of the important factors affecting the LC characteristics is their planarity. Since all compounds are neither linear nor coplanar, their enhanced mesophases will be highly affected upon mixing. Very recently, our group reported that the co-planar structures allowed for a strong parallel interaction; in addition, the long alkoxy chain length led to a strong terminal aggregation that affected the mesomorphic phases. Furthermore, the competitive terminal and lateral interactions affected the mesomorphic properties, as shown in Figure 6.

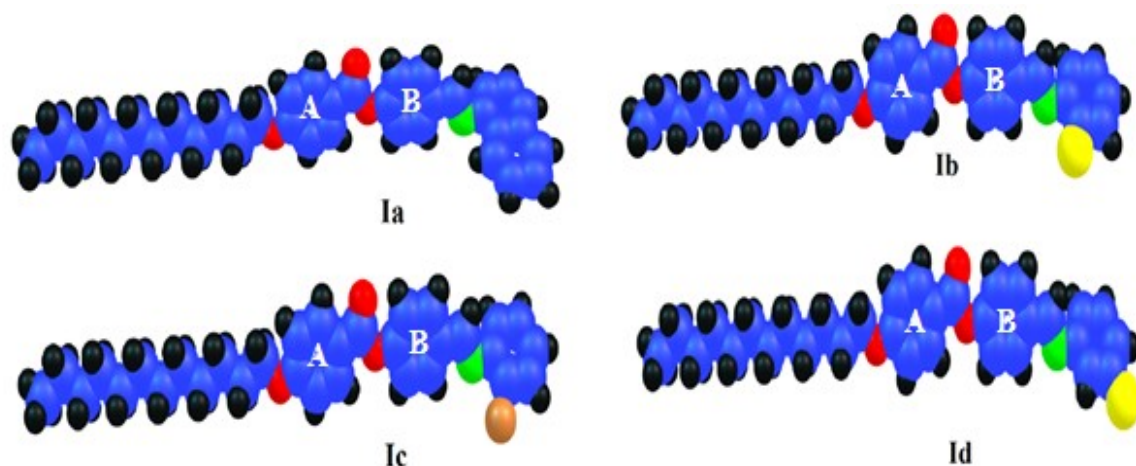


Figure 6. Optimized geometrical structures of Ia–d.

The co-planarity of the benzene rings of the individual compounds before mixing was estimated from the calculation of the twist angle ( $\theta$ ) between the planes passing through the rings (terminal = A and internal B) of the imino group (CH=N). The twist angle ( $\theta$ ) between the aromatic rings of the Schiff base derivatives varied a little depending on the type of the attached substituent. Values of the twist angles were estimated to be  $40^\circ$ ,  $41^\circ$ ,  $39^\circ$ , and  $40^\circ$  between the rings A–B for compounds Ia, Ib, Ic, and Id, respectively. The dihedral angle showed that all compounds were almost in the same degree of twisting of rings A and B. The mixing of none such co-planar compounds Ia–d improved the mesomorphic properties rather than of both individual components. The mixture of two non-co-planar compounds induced the mesophase stability and its ranges due to the formation of a certain type of interaction (perhaps  $\pi$ – $\pi$  stacking interactions) that cannot present in their individual component.

The dipole moment and the polarizability were estimated by the DFT calculations for the individual components and are summarized in Table 2. It is well known that the dimension of the present investigated materials as well as the electronic nature of the mesogenic core and the attached substituents has high impact on the polarizability [48,49]. Table 2 showed that the length of all compounds under investigation were almost the same at  $\approx 36$  Å, however, their width was not the same because of the position and size of the attached lateral groups. The space filling of the naphthyl group was higher than that of the halo derivatives; moreover, due to the size and the lower inductive effect of the Br-atom compared with the F-atom, the length of the former was higher than that of the later. The different lengths of the investigated compounds resulted in the aspect ratio L/D values, which increased in the order of Ia < Ic < Ib < Id.

Table 2. Parameters (Hartree/Particle) and dipole moment (Debye) of Ia–d.

Parameter	Ia	Ib	Ic	Id	
Polarizability $\alpha$	465.85	414.09	424.56	425.11	
Dipole Moment	4.35	4.09	4.25	6.12	
Twist angle between A-B	40	41	39	40	
Dimensions Å	Width (D)	9.51	7.89	8.76	7.82
	Length (L)	36.81	36.65	36.51	36.56
Aspect ratio (L/D)	3.87	4.65	4.17	4.68	

The halo compounds almost had the same aspect ratios of  $\approx 420$  Bohr<sup>3</sup> with little difference in the polarizability, according to the position of the F-atom. Since the polarizability is affected by the aspect ratios and the resonance as well as the inductive effect of the attached groups; it was changed from



414.09 to 425.11 Bohr<sup>3</sup> due to the electronic effect of the F-atom, which could be changed by changing its attachment position. However, the replacement of the lateral F-atom (Ib) with the benzene ring (Ia) or Br-atom (Ic) changed the polarizability, due to the impact of the aspect ratio, to  $\alpha = 465$  Bohr<sup>3</sup> for Ia and 424 Bohr<sup>3</sup> for Ic.

The dipole moment of the individual components was almost the same, except for Id, and this can be explained in the term of the orientational effect. The high dipole moment (perhaps quadrupolar) could permit a high degree of lateral interactions such as  $\pi$ - $\pi$  stacking to enhance the mesophase stabilities and their ranges.

On the other hand, the charge distribution map for the investigated components was calculated under the same basis sets according to their molecular electrostatic potential (MEP) (Figure 7). Figure 7 emphasizes that the type and the orientation of the attached polar group has a significant effect on the charge distribution. Recently, we have reported [7,9,12,16,45–47] that the mesophase range as well as its stability is highly impacted by the competitive interaction between end-to-end and side-side interaction.

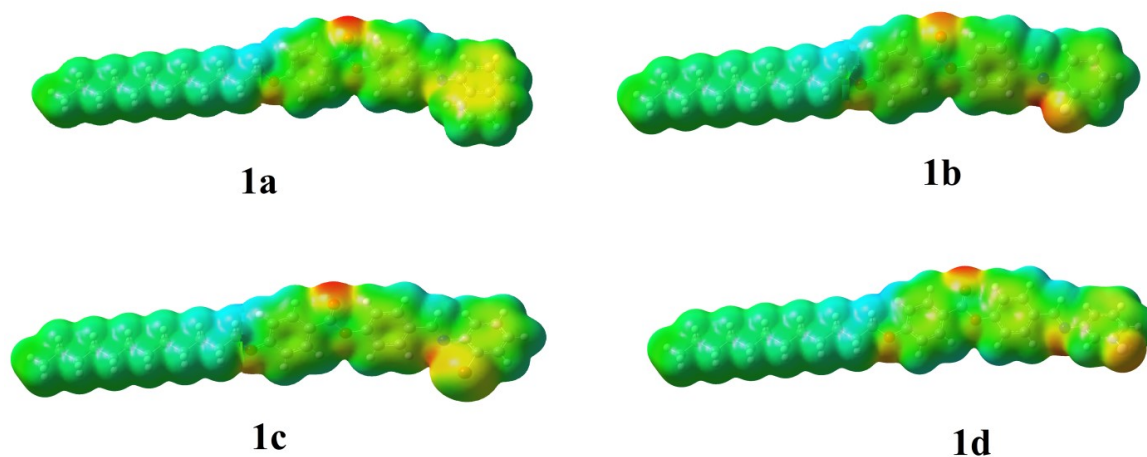


Figure 7. Molecular electrostatic potentials (MEP) of Ia–d.

From the DFT theoretical calculations, the molecular geometry and space filling of lateral groups are the most effective factors on mesomorphic behavior. Moreover, the dipole moment and orientation of lateral substituents play an important role on the mesomeric characteristics in pure and binary mixtures of the components.

#### 4. Conclusions

In the present work, three types of binary phase mixtures were designed from laterally substituted Schiff base/ester liquid crystal derivatives: the first binary system was made from two structurally different compounds with different rigidity; the second was made from two isomeric components bearing the same polar group but of different orientation; and the third one was designed from two components bearing substituents of the same orientation but of different size. Theoretical parameters for individual components were carried out by DFT calculations to study their effect on the mesomorphic characteristics of the binary mixture.

The study revealed that:

1. All prepared binary phase diagrams showed enantiotropic mesomorphic behavior.
2. Induced SmA phase was observed for the Ia/Ib system and covered all mixing compositions.
3. As usual, all binary systems showed depression in the melting temperature
4. The binary phase mixtures Ia/Ib and Ib/Id each possessed eutectic behavior, but the third Ic/Id mixture showed no eutectic compositions.

- Regular decreases in nematic-to-isotropic liquid dependency were exhibited in all binary phase diagrams.
- The estimated aspect ratios for the lateral components increased in the following order: Ia < Ic < Ib < Id.
- The polarizability was highly impacted by the dimensions and the type of lateral group.
- Id showed the highest dipole moment value (6 Debye), thus it has a high degree of lateral interactions, which impact the mesophase behavior.

**Supplementary Materials:** The following are available online at <http://www.mdpi.com/2073-4352/10/4/319/s1>, Scheme S1: Synthesis of 4-((2' or 3'-arylimino)methyl)phenyl-4''-alkoxy benzoates, Ia-d; Figure S1: DSC thermograms of binary mixture 60 mol% Ia for system Ia/Ib upon heating/cooling cycles with rate 10 °C/min; Figure S2: DSC thermograms of binary mixture 60 mol% Ib for system Ib/Id upon second heating/cooling cycles with rate 10 °C/min; Figure S3: DSC thermograms of binary mixture 60 mol% Ic for system Ic/Id upon second heating/cooling cycles with rate 10 °C/min; Figure S4: POM textures of binary mixtures upon heating (a) N phase of 60 mol% Ia for system Ic/Id at 112 °C; (b) SmA phase of 60 mol% Ia for system Ia/Ib at 84 °C; (c) N phase of 60 mol% Ia for system Ia/Ib at 101 °C.

**Author Contributions:** R.B.A., M.H., H.A.A., M.M.N., H.A.S., J.S.A., M.M.H., R.A.A. and T.A.A. designed the experiment and carried out the laboratory work; accomplished the data analysis and drafted the manuscript; and gave final approval for publication. All authors have read and agreed to the published version of the manuscript.

**Funding:** This research received no external funding.

**Conflicts of Interest:** The authors declare no conflict of interest.

## References

- Fujikake, H.; Sato, H.; Murashige, T. Polymer-stabilized ferroelectric liquid crystal for flexible displays. *Displays* **2004**, *25*, 3–8. [[CrossRef](#)]
- Ahmed, H.; Hagar, M.; Alhaddad, O. New chair shaped supramolecular complexes-based aryl nicotinate derivative; mesomorphic properties and DFT molecular geometry. *RSC Adv.* **2019**, *9*, 16366–16374. [[CrossRef](#)]
- Chen, K.-Y. Crystal Structure, Hydrogen-Bonding Properties, and DFT Studies of 2-((2-(2-Hydroxyphenyl)benzo[d]thiazol-6-yl) methylene) malononitrile. *Mol. Cryst. Liq. Cryst.* **2015**, *623*, 285–296. [[CrossRef](#)]
- Shoji, M.; Tanaka, F. Theoretical study of hydrogen-bonded supramolecular liquid crystals. *Macromolecules* **2002**, *35*, 7460–7472. [[CrossRef](#)]
- Sundaram, S.; Jayaprakasam, R.; Dhandapani, M.; Senthil, T.; Vijayakumar, V. Theoretical (DFT) and experimental studies on multiple hydrogen bonded liquid crystals comprising between aliphatic and aromatic acids. *J. Mol. Liq.* **2017**, *243*, 14–21. [[CrossRef](#)]
- Al-Mutabagani, L.; Alshabanah, L.A.; Ahmed, H.; Hagar, M.; Al-Ola, K.A.A. New Symmetrical U- and Wavy-shaped Supramolecular H-bonded Systems; Geometrical and Mesomorphic Approaches. *Molecules* **2020**, *25*, 1420. [[CrossRef](#)]
- Hagar, M.; Ahmed, H.; Saad, G. New calamitic thermotropic liquid crystals of 2-hydroxypyridine ester mesogenic core: Mesophase behaviour and DFT calculations. *Liq. Cryst.* **2020**, *47*, 114–124. [[CrossRef](#)]
- Ahmed, N.H.; Saad, G.R.; Ahmed, H.A.; Hagar, M. New wide-stability four-ring azo/ester/Schiff base liquid crystals: Synthesis, mesomorphic, photophysical, and DFT approaches. *RSC Adv.* **2020**, *10*, 9643–9656. [[CrossRef](#)]
- Alhaddad, O.; Ahmed, H.; Hagar, M. Experimental and Theoretical Approaches of New Nematogenic Chair Architectures of Supramolecular H-Bonded Liquid Crystals. *Molecules* **2020**, *25*, 365. [[CrossRef](#)]
- Nafee, S.S.; Ahmed, H.A.; Hagar, M. New architectures of supramolecular H-bonded liquid crystal complexes based on dipyrindine derivatives. *Liq. Cryst.* **2020**, 1–14. [[CrossRef](#)]
- Nafee, S.S.; Hagar, M.; Ahmed, H.A.; El-Shishtawy, R.M.; Raffah, B.M. The synthesis of new thermal stable schiff base/ester liquid crystals: A computational, mesomorphic, and optical study. *Molecules* **2019**, *24*, 3032. [[CrossRef](#)] [[PubMed](#)]
- Ahmed, H.; Hagar, M.; Saad, G. Impact of the proportionation of dialkoxy chain length on the mesophase behaviour of Schiff base/ester liquid crystals; experimental and theoretical study. *Liq. Cryst.* **2019**, *46*, 1611–1620. [[CrossRef](#)]

13. Ahmed, H.A.; Hagar, M.; Alhaddad, O.A. Phase behavior and DFT calculations of laterally methyl supramolecular hydrogen-bonding complexes. *Crystals* **2019**, *9*, 133. [[CrossRef](#)]
14. Hagar, M.; Ahmed, H.; El-Sayed, T.; Alnoman, R. Mesophase behavior and DFT conformational analysis of new symmetrical diester chalcone liquid crystals. *J. Mol. Liq.* **2019**, *285*, 96–105. [[CrossRef](#)]
15. Alnoman, R.; Ahmed, H.A.; Hagar, M. Synthesis, optical, and geometrical approaches of new natural fatty acids' esters/Schiff base liquid crystals. *Molecules* **2019**, *24*, 4293. [[CrossRef](#)] [[PubMed](#)]
16. Hagar, M.; Ahmed, H.; Alhaddad, O. New azobenzene-based natural fatty acid liquid crystals with low melting point: Synthesis, DFT calculations and binary mixtures. *Liq. Cryst.* **2019**, *46*, 2223–2234. [[CrossRef](#)]
17. Ahmed, H.; Hagar, M.; Alhaddad, O. Mesomorphic and geometrical orientation study of the relative position of fluorine atom in some thermotropic liquid crystal systems. *Liq. Cryst.* **2019**, 1–10. [[CrossRef](#)]
18. Zaki, A.A.; Ahmed, H.; Hagar, M. Impact of fluorine orientation on the optical properties of difluorophenylazophenyl benzoates liquid crystal. *Mater. Chem. Phys.* **2018**, *216*, 316–324. [[CrossRef](#)]
19. Weissflog, W.; Demus, D. Compounds with lateral long-chain substituents—A new molecule structure concept for thermotropic liquid crystals. *Cryst. Res. Technol.* **1983**, *18*, K21–K24. [[CrossRef](#)]
20. Weissflog, W.; Demus, D. Thermotropic liquid crystalline compounds with lateral long-chain substituents (II): Synthesis and liquid crystalline properties of 1, 4-Bis [4-substituted-benzoyloxy]-2-n-alkylbenzenes. *Cryst. Res. Technol.* **1984**, *19*, 55–64. [[CrossRef](#)]
21. Weissflog, W.; Demus, D. New lateral long-chain substituted liquid crystals. *Mol. Cryst. Liq. Cryst.* **1985**, *129*, 235–243. [[CrossRef](#)]
22. Ahmed, H.; Hagar, M.; Aljuhani, A. Mesophase behavior of new linear supramolecular hydrogen-bonding complexes. *RSC Adv.* **2018**, *8*, 34937–34946. [[CrossRef](#)]
23. Hagar, M.; Ahmed, H.; Saad, G. Mesophase stability of new Schiff base ester liquid crystals with different polar substituents. *Liq. Cryst.* **2018**, *45*, 1324–1332. [[CrossRef](#)]
24. Dave, J.; Patel, P.; Vasanth, K. Mixed mesomorphism in binary systems forming smectic-nematic phases. *Mol. Cryst.* **1969**, *8*, 93–100. [[CrossRef](#)]
25. Dave, J.S.; Menon, M.R.; Patel, P.R. Chiral phases induced by doping nonmesogenic component into mesogenic esters. *Mol. Cryst. Liq. Cryst.* **2003**, *392*, 83–95. [[CrossRef](#)]
26. Vora, R.; Gupta, R.; Patel, K. Exhibition of induced mesophases in the binary systems where one or both the components are non-mesogenic. *Mol. Cryst. Liq. Cryst.* **1991**, *209*, 251–263. [[CrossRef](#)]
27. Fujimura, S.; Yamamura, Y.; Hishida, M.; Nagatomo, S.; Saito, K. Reentrant nematic phase in 4-alkyl-4'-cyanobiphenyl (n CB) binary mixtures. *Liq. Cryst.* **2014**, *41*, 927–932. [[CrossRef](#)]
28. Prasad, A.; Das, M.K. Determination of elastic constants of a binary system (7CPB+ 9. CN) showing nematic, induced smectic Ad and re-entrant nematic phases. *Liq. Cryst.* **2014**, *41*, 1261–1268. [[CrossRef](#)]
29. Salud, J.; Lopez, D.; Diez-Berart, S.; de la Fuente, M. Tests of the tricritical point in the SmA-to-N phase transition of binary mixtures of butyloxybenzylidene octylaniline and hexyloxybenzylidene octylaniline. *Liq. Cryst.* **2013**, *40*, 293–304. [[CrossRef](#)]
30. Prajapati, A.K.; Patel, N.S.; Lad, V.G. Induction of chirality by doping mesogens with non-mesogenic chiral dopant. *Mol. Cryst. Liq. Cryst. Sci. Technol. Sect. A. Mol. Cryst. Liq. Cryst.* **2000**, *348*, 41–51. [[CrossRef](#)]
31. Vora, R.; Rajput, S. Binary mesogenic systems comprised of ester mesogens and non-mesogens. *Mol. Cryst. Liq. Cryst.* **1991**, *209*, 265–277. [[CrossRef](#)]
32. Govindaiah, T.; Nagappa; Sathyanarayana, P.; Mahadeva, J.; Sreepad, H. Induced chiral smectic phase in mixtures of mesogenic and non-mesogenic compounds. *Mol. Cryst. Liq. Cryst.* **2011**, *548*, 55–60. [[CrossRef](#)]
33. Lohar, J.; Dave, J.S., Jr. Emergence of smectic mesophase in binary mixtures of pure nematogens. *Mol. Cryst. Liq. Cryst.* **1983**, *103*, 181–192. [[CrossRef](#)]
34. Sarkar, S.D.; Choudhury, B. Study of binary mixtures of two liquid crystalline samples showing induced smectic phase. *Assam Univ. J. Sci. Technol.* **2010**, *5*, 167–168.
35. Ahmed, H.; Naoum, M. Mesophase behavior of binary and ternary mixtures of benzoic acids bearing terminal substituents of different polarity and chain-lengths. *Thermochim. Acta* **2014**, *575*, 122–128. [[CrossRef](#)]
36. Alhaddad, O.A.; Ahmed, H.A.; Hagar, M.; Saad, G.R.; Al-Ola, A.; Khulood, A.; Naoum, M.M. Thermal and Photophysical Studies of Binary Mixtures of Liquid Crystal with Different Geometrical Mesogens. *Crystals* **2020**, *10*, 223. [[CrossRef](#)]
37. Ahmed, H.; Naoum, M.; Saad, G. Mesophase behaviour of 1: 1 mixtures of 4-n-alkoxyphenylazo benzoic acids bearing terminal alkoxy groups of different chain lengths. *Liq. Cryst.* **2016**, *43*, 1259–1267. [[CrossRef](#)]

38. Naoum, M.; Mohammady, S.; Ahmed, H. Lateral protrusion and mesophase behaviour in pure and mixed states of model compounds of the type 4-(4'-substituted phenylazo)-2-(or 3-) methyl phenyl-4'-alkoxy benzoates. *Liq. Cryst.* **2010**, *37*, 1245–1257. [[CrossRef](#)]
39. Mohamady, S.Z.; Nessim, R.I.; Shehab, O.R.; Naoum, M.M. Effect of steric factor on mesomorphic stability, II: Binary mixtures of homologues of 4-(4'-substituted phenylazo)-1-naphthyl-4''-alkoxybenzoates. *Mol. Cryst. Liq. Cryst.* **2006**, *451*, 53–64. [[CrossRef](#)]
40. Naoum, M.; Fahmi, A.; Alaasar, M.; Abdel-Aziz, M. Effect of lateral substitution of different polarity on the mesophase behaviour in pure and mixed states of 4-(4'-substituted phenylazo)-2-substituted phenyl-4'-alkoxy benzoates. *Liq. Cryst.* **2011**, *38*, 391–405. [[CrossRef](#)]
41. Frisch, M.; Trucks, G.; Schlegel, H.B.; Scuseria, G.; Robb, M.; Cheeseman, J.; Scalmani, G.; Barone, V.; Mennucci, B.; Petersson, G. *Gaussian 09, Revision A. 02*; Gaussian Inc.: Wallingford, CT, USA, 2009; p. 200.
42. Dennington, R.; Keith, T.; Millam, J. *GaussView, Version 5*; Semicem Inc.: Crieff, UK, 2009.
43. Ahmed, H.; Hagar, M.; El-Sayed, T.B.; Alnoman, R. Schiff base/ester liquid crystals with different lateral substituents: Mesophase behaviour and DFT calculations. *Liq. Cryst.* **2019**, *46*, 1–11. [[CrossRef](#)]
44. Naoum, M.M.; Saad, G.R.; Nessim, R.I.; Abdel-Aziz, T.A.; Seliger, H. Effect of molecular structure on the phase behaviour of some liquid crystalline compounds and their binary mixtures II. 4-Hexadecyloxyphenyl arylates and aryl 4-hexadecyloxy benzoates. *Liq. Cryst.* **1997**, *23*, 789–795. [[CrossRef](#)]
45. Nafee, S.S.; Ahmed, H.; Hagar, M. Theoretical, experimental and optical study of new thiophene-based liquid crystals and their positional isomers. *Liq. Cryst.* **2020**, 1–12. [[CrossRef](#)]
46. Hagar, M.; Ahmed, H.; Saad, G. Synthesis and mesophase behaviour of Schiff base/ester 4-(arylideneamino) phenyl-4''-alkoxy benzoates and their binary mixtures. *J. Mol. Liq.* **2019**, *273*, 266–273. [[CrossRef](#)]
47. Nafee, S.S.; Hagar, M.; Ahmed, H.A.; Alhaddad, O.; El-Shishtawy, R.M.; Raffah, B.M. New two rings Schiff base liquid crystals; ball mill synthesis, mesomorphic, Hammett and DFT studies. *J. Mol. Liq.* **2019**, *299*, 112161. [[CrossRef](#)]
48. Kim, S.N.; Kastelic, J.R. Use of Liquid Crystal Polymer Particulates Having a High Aspect Ratio in Polymeric Molding Resins to Suppress Melt Dripping. U.S. Patent 4,439,578, 27 March 1984.
49. Sengupta, A.; Tkalec, U.; Ravnik, M.; Yeomans, J.M.; Bahr, C.; Herminghaus, S. Liquid crystal microfluidics for tunable flow shaping. *Phys. Rev. Lett.* **2013**, *110*, 048303. [[CrossRef](#)]



© 2020 by the authors. Licensee MDPI, Basel, Switzerland. This article is an open access article distributed under the terms and conditions of the Creative Commons Attribution (CC BY) license (<http://creativecommons.org/licenses/by/4.0/>).